Journal of Electroanalytical Chemistry 649 (2010) 171–176

Contents lists available at ScienceDirect

Journal of Electroanalytical Chemistry

journal homepage: www.elsevier.com/locate/jelechem

In situ microscope FTIR spectroscopic studies of interfacial reactions of Sn–Co alloy film anode of lithium ion battery

Jun-Tao Li [a,b], Shu-Ru Chen [b], Fu-Sheng Ke [b], Guo-Zhen Wei [b], Ling Huang [b], Shi-Gang Sun [b,*]

[a] School of Energy Research, Xiamen University, Xiamen 361005, China
[b] State Key Laboratory of Physical Chemistry of Solid Surfaces, Department of Chemistry, College of Chemistry and Chemical Engineering, Xiamen University, Xiamen 361005, China

ARTICLE INFO

Article history:
Received 15 October 2009
Received in revised form 4 March 2010
Accepted 29 March 2010
Available online 3 April 2010

This paper is dedicated to the 65th birthday of Prof. Jacek Likpowski

Keywords:
In situ MFTIRS
Interfacial reactions
Sn–Co alloy thin film
Anode
SEI layer
Lithium ion battery

ABSTRACT

Sn–Co alloy thin films with high IR reflectivity were prepared by electroplating on a copper substrate and served as anodes of lithium ion battery. The interfacial properties of the Sn–Co alloy anode in an electrolyte of 1 M $LiPF_6$/EC + DMC (1:1, vol.%) during discharge/charge (or lithiation/delithiation) processes were investigated by using in situ microscope Fourier transform infrared reflection spectroscopy (in situ MFTIRS). The results demonstrated that the solvation/desolvation reactions of lithium ions with solvent molecules in discharge/charge processes vary with the concentration of both solvated and free solvent molecules, leading to the shift of C=O, C–O and C–H IR bands. The effect of solvation/desolvation, which provides a possibility to probe the lithiation/delithiation processes by in situ MFTIRS, is observed and analyzed clearly. The solid electrolyte interphase (SEI) layer on a cycled Sn–Co alloy anode has also been investigated by ex situ MFTIRS, which determined that the main chemical composition of the SEI layer is $ROCO_2Li$. The current studies are of significance in understanding the interfacial reactions involving in lithium ion battery at molecular level.

1. Introduction

Sn anode exhibits a super specific capacity (993 mA h g^{-1}), and therefore attracts extensive attentions as an alternative material to carbon anodes of lithium ion batteries (LIBs). The Sn anode suffers nevertheless a high degree of volume expansion/contraction during lithium alloying/dealloying reactions, resulting in a poor cycle performance [1]. To improve the cycleability of Sn anode, intensive efforts have been made through the synthesis of nano-sized/porous materials [2,3], or by use of Sn-based intermetallic alloys with inactive host matrix. It has shown that the inactive component can buffer, to some extent, the volume change caused by Sn component and thus increases the cycling stability. Many Sn-based intermetallic alloys such as Sn–Co [4], Sn–Ni [5], Sn–Cu [6] and Sn–Sb [7] were investigated. Though electrochemical properties of these Sn-based alloys have been improved effectively, the interfacial reactions were rarely reported.

The reactions occurring in the interfaces between electrodes and nonaqueous electrolyte include insertion/extraction of lithium ion, decomposition of electrolyte and formation of solid electrolyte interphase (SEI) layer. The interfacial properties are the key issue relating to the cycling ability, life time, chemical and physical stability and reversible capacity of a LIB. In addition, the interfacial reactions on Sn-based electrodes are evidently different from those of carbonaceous anodes that were intensively studied by using various methods. The investigation of the interfacial phenomena of Sn-based alloy at a molecule level is of importance for the development of LIBs.

The applications of Fourier transform infrared spectroscopy (FTIRS) in studies of LIBs are significant, since it can provide information at molecular level [8]. The chemical compositions of SEI layers on various materials of LIBs, aged or cycled in different electrolytes, were examined by ex situ FTIRS [9–13]. In situ FTIRS investigations focusing on the reduction/oxidation of various electrolytes were carried on LIBs electrodes [14–18] or nonactive [19,20] materials. On the traditional LIBs powder electrode materials, however, the strong absorption of IR light makes it difficult to be studied by FTIRS due to a low reflectivity for incident IR radiation in most cases. Fortunately, Sn or Sn-based alloy thin film electrodes prepared by electroplating have a high IR reflectivity, so that IR spectra with high signal-to-noise ratio can be obtained, which provides detail information concerning the evolutions of species involving in the interfacial reactions.

We have studied the interfacial reactions of a Sn anode by using a FTIR microscope system to perform in situ infrared reflection measurements [21], and demonstrated that the processes of lithium insertion/extraction can be well-characterized by in situ

* Corresponding author. Tel.: +86 592 218 0181; fax: +86 592 2183047.
E-mail address: sgsun@xmu.edu.cn (S.-G. Sun).

1572-6657/$ - see front matter © 2010 Elsevier B.V. All rights reserved.
doi:10.1016/j.jelechem.2010.03.032

microscope FTIR spectroscopy (MFTIRS) through the solvation/desolvation effects. In this paper, Sn–Co alloy thin film electrodes were further prepared by electroplating. Interfacial reactions and SEI layer on the Sn–Co alloy thin film anodes were investigated by both in situ MFTIRS and ex situ MFTIRS. The lithiation/delithiation processes of lithium with Sn–Co anode, the solvation/desolvation of lithium ions with solvent molecules and the chemical composition of SEI layer were characterized and analyzed.

2. Experimental section

2.1. Microscope Fourier transform infrared spectroscopy (MFTIRS)

MFTIRS studies were carried out on a Nexus 870 FTIR spectrometer (Nicolet) and a microscope (IR-Plan® Advantage, Spectra-Tech Inc.) equipped with an HgCdTe detector (MCT-A) cooled with liquid N_2. The in situ MFTIRS cell and the array of copper substrate electrodes were detailed in our previous paper [21]. A KBr disc was used as IR window. Different structures or composition of metal/alloy thin films can be deposited electrochemically on Cu substrates of the array. In this study, interfacial reactions of Sn–Co alloy thin film anode and copper substrate electrode were compared under the same experiment conditions, by using lithium foils as both reference and counter electrodes. The in situ FTIR spectrum is defined as:

$$\frac{\Delta R}{R}(E_S) = \frac{R(E_S) - R(E_R)}{R(E_R)} \quad (1)$$

where $R(E_S)$ and $R(E_R)$ are single-beam spectra collected at sample potential E_S and reference potential E_R, respectively. The E_S was varied step by step with an interval of 0.10 V, and single-beam spectrum was collected at each E_S after a polarization of 800 s at the E_S in order to establish a stable interface. Each single-beam spectrum was acquired by collecting and coadding 400 interferograms at a spectral resolution of 4 cm^{-1}.

Ex situ MFTIRS measurements were carried out on a cycled sample in the same sealed IR cell without electrolyte. Before this measurement, a cycled Sn–Co alloy thin film anode was emerged from electrolyte, rinsed by DMC, and kept in a vacuum for 24 h. It was then transferred to the sealed IR cell. All above operations were carried out inside a glove box filled up with pure Ar gas. The result spectrum is calculated also by using Eq. (1), where the $R(E_S)$ and $R(E_R)$ stand for single-beam spectra collected on the cycled and pristine Sn–Co alloy thin films, respectively. Each single-beam spectrum was acquired by collecting and coadding 200 interferograms with 4 cm^{-1} spectral resolution.

All battery cells in this study were assembled in the Ar-filled glove box. Measurements were carried out at room temperature. A 263 potentiostat/galvanostat (EG&G) was employed to control electrode potential. The electrolyte composes of a solution of 1 M $LiPF_6$ in a mixture of ethylene carbonate (EC)/dimethyl carbonate (DMC) (1:1, vol.%), and was purchased from Guotai-huarong New Chemical Materials Co., Ltd. (Zhangjiagang, China). The coin cells were galvanostatically discharged and charged on a battery test system (NEWARE BTS-610, Neware Technology Co., Ltd., China). The potentials reported in this paper were referred to the Li^+/Li electrode potential scale.

2.2. Preparation of Sn–Co alloy thin film electrodes

Electroplating of Sn–Co alloy films on copper substrate eletrodes of the array (dimeter = 1.1 mm, for both cyclic voltammetry and MFTIRS studies) and copper foils (dimeter = 16 mm, thickness = 0.1 mm, for galvanostatically discharge–charge tests only)

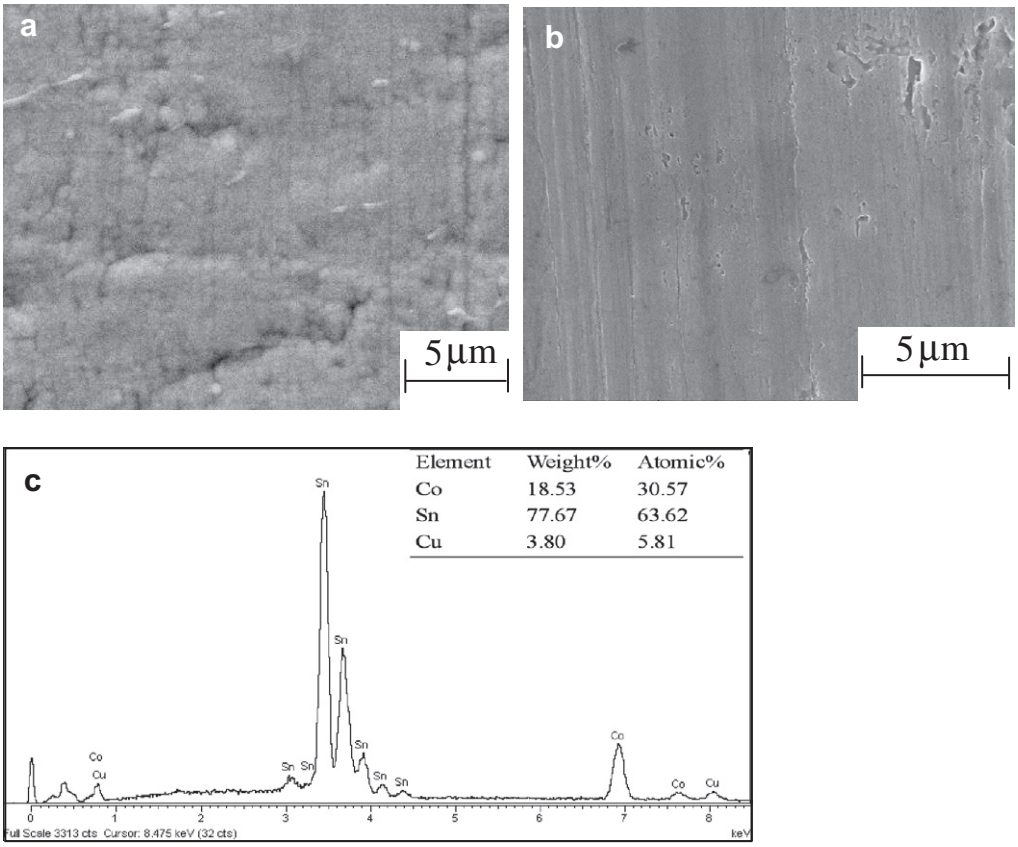

Fig. 1. SEM images of (a) Sn–Co alloy thin film electrode, (b) copper substrate electrode and (c) EDX analysis of Sn–Co alloy thin film electrode.

were carried out in a plating bath containing 75 g L^{-1} $Na_2SnO_3{\cdot}3H_2O$, 2.5 g L^{-1} $CoCl_2{\cdot}6H_2O$, 150 g L^{-1} $C_4H_4O_6KNa{\cdot}4H_2O$, and 20 g L^{-1} $K_3C_6H_5O_7{\cdot}H_2O$. The bath temperature was kept at 55 °C and the pH value of solution was adjusted to 7.5 by adding HCl into the solution. Titanium foil was served as counter electrode. A constant current density of 0.7 A dm^{-2} was flowed for 20 min. After electroplating, the prepared electrode was transferred to an anhydrous ethanol bath and sonicated for 1 min, and then dried at 105 °C under 10^{-3} Torr for 12 h in vacuum. Scanning electron microscopy (SEM) observation and energy dispersive X-ray spectroscopy (EDS) analysis, shown in Fig. 1, have revealed that smooth Sn–Co alloy thin film was produced, with a Sn atomic ratio of 63.6% and Co atomic ratio of 30.6%. The atomic ratio of Sn–Co is about 2:1.

3. Results and discussion

3.1. Electrochemical studies

Fig. 2 shows the first three consecutive cyclic voltammograms (CVs) of Sn–Co alloy thin film electrode recorded at scan rate 0.5 mV s^{-1} in lithiation/delithiation potential region. In the first negative-going potential scan (NGPS), alloying of lithium ion with Sn–Co anode starts at about 0.4 V and gives rise to a cathodic current peak at 0.06 V, which positively shifts to 0.22 V in the subsequent NGPSs. In the positive-going potential scan (PGPS), anodic current peaks at 0.50 and *ca.* 0.6 V are observed and assigned to the extraction of lithium from Li_xSn phase. These peaks appear at the same potentials in the following PGPSs.

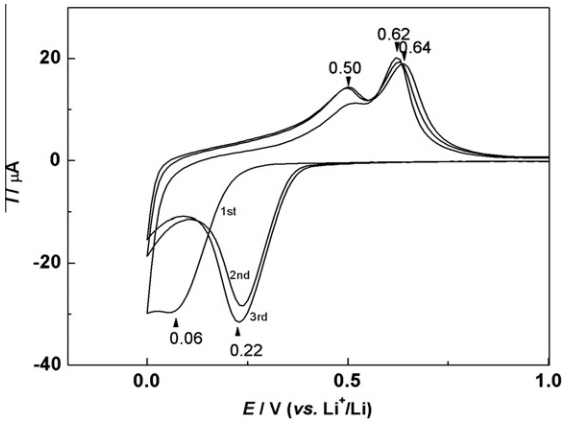

Fig. 2. Cyclic voltammograms of the first three consecutive cycles of Sn–Co alloy thin film anode in 1 M $LiPF_6$/EC + DMC (1:1, vol.%). Scan rate: 0.50 mV s^{-1}.

Sn–Co thin film anode was tested for its cycling ability using constant current cycling over a voltage range of 0.02–1.5 V. The discharge–charge voltage profiles for the 1st, 2nd, 3rd, 15th and 25th cycles are displayed in Fig. 3a. Alloying and dealloying of lithium in a half cell are defined as discharge and charge processes, respectively. The potential drops rapidly to a plateau of 0.24 V, and then decreases gradually to 0.02 V in the first discharge process. The plateau at 0.24 V and the gentle incline from that to 0.02 V correspond to the lithiation process of various stages of the Sn–Co thin film anode. In the 2nd, 3rd and 15th cycles, the potential plateau at 0.24 V increases to 0.35 V, while this plateau disappears in the 25th cycle and only a slope from 0.5 to 0.02 V is observed. This voltage fluctuation may be resulted from the irreversible decomposition reaction of Sn–Co alloy to Co and Sn [22]. However, the lithiation potential of Sn–Co alloy still differs from that of pure Sn from a thermodynamic consideration point of view. In the course of lithium dealloying, the variation of curves from 1st to 25th cycles are similar but with different capacity. In all charge curves, the potential increases gradually to about 0.24 V and reaches a plateau at 0.59 V, then rises rapidly to 1.50 V. The potential plateau and the gentle slope are ascribed to the process of lithium extraction from Li_xSn phase.

The cycling performance profiles of Sn–Co alloy thin film in the first 25 cycles at a current rate of 50 mA g^{-1} are illustrated in Fig. 3b. Sn–Co alloy thin film anode delivers a first discharge capacity of 520 mA h g^{-1} and a charge capacity of 437 mA h g^{-1}, yielding a columbic efficiency of 84%. The discharge capacity is varied in the following three stages: the first stage is from 1st to 6th cycle, where the discharge capacity decreases slightly and holds a value of 372 mA h g^{-1} at the 6th cycle. The second stage lies in the 7th to12th cycles, where the capacity maintains stable. The following third stage is varied from 13th to 25th cycle, where the capacity decreases quickly and is declined to 217 mA h g^{-1} in the 25th cycle. The capacity decline is mainly caused by the volume effects during the lithiation/delithiation processes. The general reaction during alloying/dealloying of lithium with Sn–Co alloy thin film electrode may be written as:

$$CoSn_2 + 2xLi^+ + 2xe^- \rightleftarrows 2Li_xSn + Co \quad (x < 4.4) \tag{2}$$

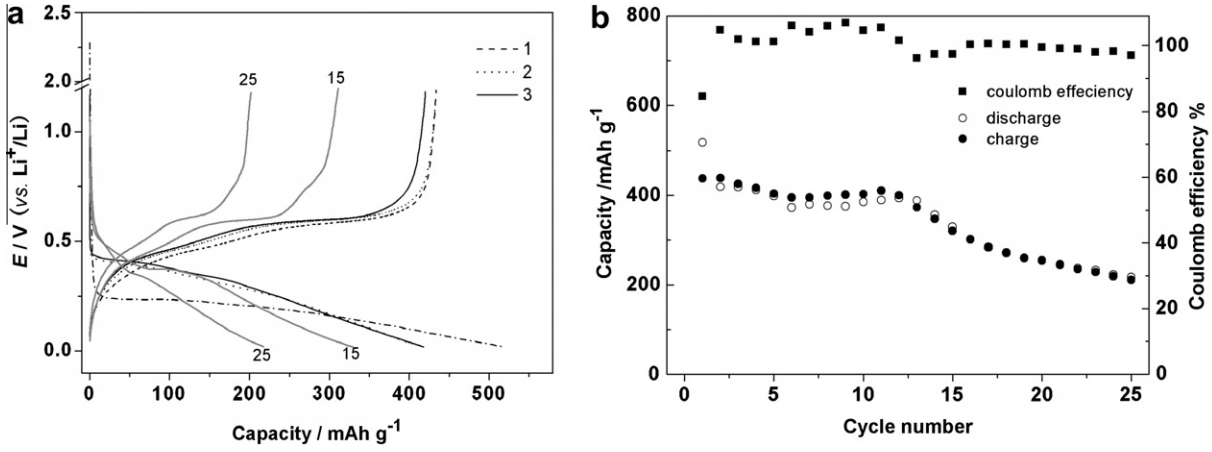

Fig. 3. Variations of (a) galvanostatic discharge–charge and (b) capacity versus cycle number of Sn–Co alloy thin film anode in 1 M $LiPF_6$/EC + DMC (1:1, vol.%). Current rate: 50 mA g^{-1}.

3.2. In situ MFTIRS studies

Fig. 4 illustrates the in situ MFTIR spectra recorded on the Sn–Co alloy thin film anode during the first lithiation process. The $R(E_R)$ is set at 0.70 V, where lithiation does not take place. Downward and upward IR bands are observed obviously in potential range of 0.2–0.02 V, indicating the variation of related species in the thin layer between electrode and IR window. As the result spectra were calculated by using Eq. (1), the downward bands in spectra indicate the increase or formation of correlated species, while the upward ones signify the decrease or disappearance of related species. When E_S is cathodically polarized from 0.7 to 0.02 V, lithium ions desolvate firstly from solvated solvent molecules, and then alloy with Sn–Co anode. As a result, if taking account of solvation/desolvation reactions in the lithiation/delithiation processes [23], the Eq. (2) could be rewritten as:

$$CoSn_2 + 2xLi(sol)_n^+ + 2xe^- \rightleftarrows 2Li_xSn + Co + 2nxsol \quad (x < 4.4) \tag{3}$$

where $Li(sol)_n^+$ is the solvated solvent molecule with lithium ion, and the sol stands for the free solvent molecule (EC, DMC) in electrolyte. As a consequence, the concentration of free solvent molecule increases while that of $Li(sol)_n^+$ decreases in lithiation process. So the downward bands appeared in the in situ MFTIR spectra correspond to the increase of free solvent molecules, meanwhile the upward bands imply the decrease of $Li(sol)_n^+$. In comparison with free solvent molecule, when solvent exists as the form of $Li(sol)_n^+$ the C=O bond is weakened, while the C–O bond is strengthened, due to the coordination of $Li^+\cdots O{=}C$ [24], (see the schematic diagram in Fig. 5). The IR absorption of asymmetric stretching of C=O band ($\upsilon_{as,C=O}$) in $Li(sol)_n^+$ is therefore red-shifted, while that of C–O (υ_{C-O}) is blue-shifted [25,26].

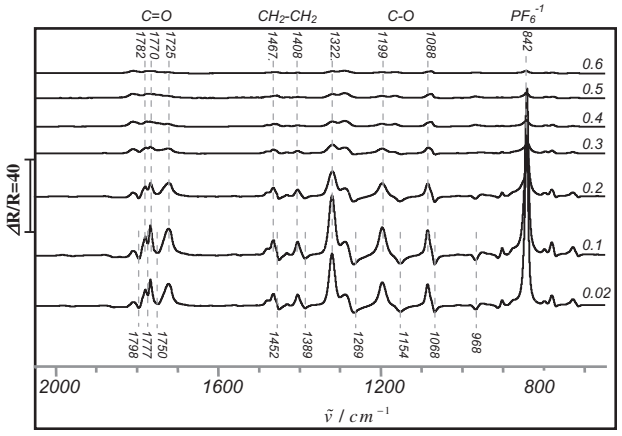

Fig. 4. In situ MFTIR spectra of Sn–Co alloy thin film anode in 1 M $LiPF_6$/EC + DMC (1:1, vol.%) in the lithiation process. E_S values are indicated in the spectra. All spectra are calculated by setting 0.70 V as reference potential.

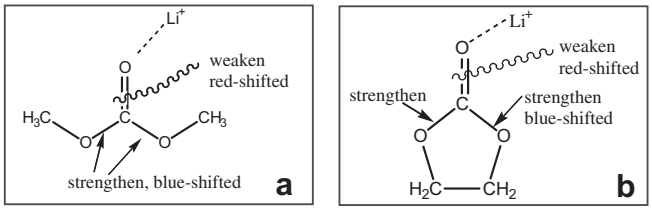

Fig. 5. Schematic illustration of molecule structures of the solvated DMC (a) and EC (b) with lithium ions.

The downward bands at 1798 and 1777 cm^{-1} are attributed to ($\upsilon_{as,C=O}$) of free EC, and the band at 1750 cm^{-1} to ($\upsilon_{as,C=O}$) of free DMC [10]. The upward peaks at 1782, 1770 and 1725 cm^{-1} can be assigned to ($\upsilon_{as,C=O}$) of $Li(sol)_n^+$. The IR bands ascribed to (υ_{C-O}) of free DMC and EC appear near 1269, 1154 and 1068 cm^{-1} in downward direction, while those bands of $Li(sol)_n^+$ are upward at higher wavenumbers of 1322, 1199 and 1088 cm^{-1}. The bands at 1467 and 1408 cm^{-1} may be ascribed to IR absorption of C–H bond in $Li(sol)_n^+$, and the downward bands at 1452 and 1398 cm^{-1} are attributed to C–H band of free solvent molecule. A strong upward band observed at 842 cm^{-1} is assigned to IR absorption of PF_6^- anions [27] duo to their diffusion from the thin layer into bulk solution to maintain electric balance of the thin layer in the lithiation process.

Fig. 6 compares in situ MFTIR spectra of Sn–Co alloy thin film anode recorded in anodic and those in cathodic polarization. The result spectrum of each E_S is calculated by using the Eq. (1) and setting the single-beam spectrum collected at its previous neighboring potential as $R(E_R)$. It is interesting to observe that IR bands in the spectra collected in anodic and cathodic polarization at the same potential show opposite direction at the same wavenumber, signifying a reversible process, i.e. the solvation of lithium ion with solvent molecule in dealloying reaction and the desolvation in alloying reaction are reversible. Different intensities of IR bands are nevertheless observed. It may indicate that the lithiation and delithiation processes take place in different potential ranges, since the IR band intensity corresponds to the degree of variations of

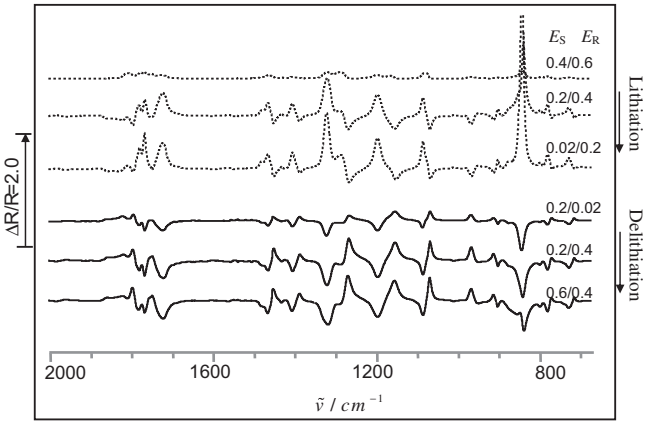

Fig. 6. Comparison of in situ MFTIR spectra of Sn–Co alloy thin film anode in 1 M $LiPF_6$/EC + DMC (1:1, vol.%) during the lithiation/delithiation processes.

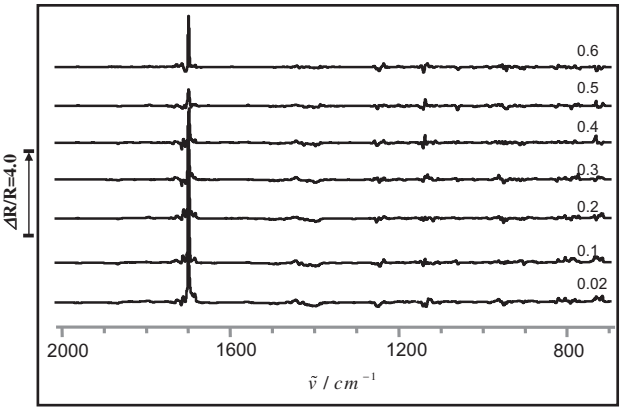

Fig. 7. In situ MFTIR spectra of Cu electrode in 1 M $LiPF_6$/EC + DMC (1:1, vol.%). E_S values are indicated in the spectra. All spectra are calculated by setting 0.70 V as reference potential.

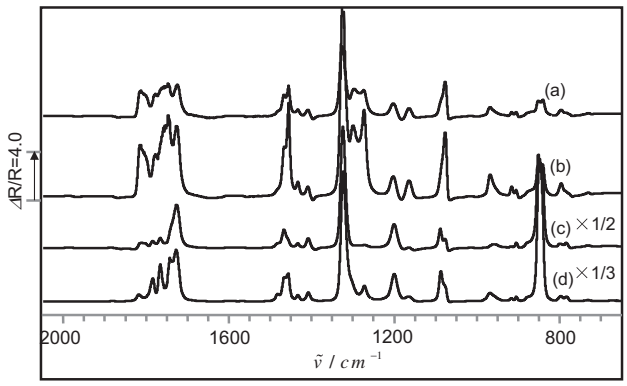

Fig. 8. Transmission FTIR spectra of (a) 0.75 M, (b) 0.50 M, (c) 0.25 M, (d) 0.10 M $LiPF_6$/EC + DMC (1:1, vol.%), the spectrum of 1 M $LiPF_6$/EC + DMC (1:1, vol.%) is setting as reference spectrum.

spectra at two neighboring potentials, which is induced by interfacial reactions.

To confirm the above analysis concerning IR properties arising from interfacial reactions of Sn–Co thin film anode during alloying/dealloying processes, in situ MFTIR spectra shown in Fig. 7 were recorded on a copper electrode of the array under the same experiment conditions used in the study of Sn–Co alloy thin film anode. Significant changes of IR bands (upward and downward peaks) were absent in the spectra recorded with Cu electrode. Since copper is nonactive for alloying with lithium ions in cathodic polarization, the desolvation of lithium ions from solvent molecule does not take place. As a consequence, the concentration of $Li(sol)_n^+$ and free solvent molecules in the thin layer between IR windows and Cu electrode do not change with electrode potential variation.

The concentration change of related species during lithiation/delithiation processes was further simulated experimentally by altering the $LiPF_6$ concentration in electrolyte solution. The transmission FTIR spectra of electrolyte with different concentration of $LiPF_6$ were collected and compared in Fig. 8. The result spectra are calculated again using Eq. (1) by setting spectrum of 1 M $LiPF_6$/EC + DME (1:1, vol.%) as the reference spectrum. Along with decreasing concentration of $LiPF_6$, the IR features of transmission spectra are similar with those of in situ spectra collected in the alloying process, since the change of related species are similar with those in the thin layer between IR windows and Sn–Co alloy electrode during the lithiation process.

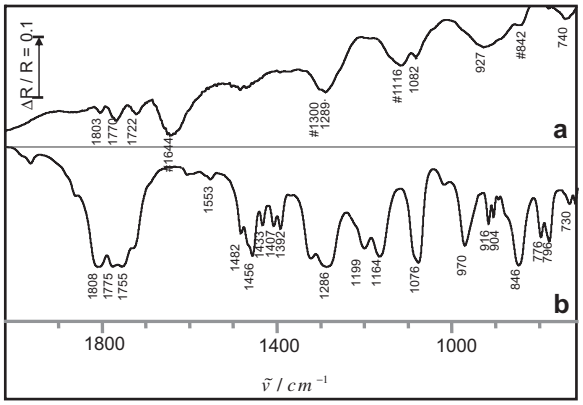

Fig. 9. (a) Ex situ MFTIRS of a cycled Sn–Co alloy thin film electrode in 1 M $LiPF_6$/EC + DMC (1:1, vol.%) and (b) transmission IR spectrum of 1 M $LiPF_6$/EC + DMC (1:1, vol.%).

3.3. Ex situ MFTIRS

Fig. 9a demonstrates ex situ MFTIR spectra recorded on a Sn–Co thin film anode that has been treated by five CV cycles between 2.70 and 0.02 V in a three-electrode glass cell. For comparison, transmission FTIR spectrum of electrolyte of 1 M $LiPF_6$/EC + DMC (1:1, vol.%) is also shown (Fig. 9b). The bands at 1803, 1770, 1722, 1289 and 1082 cm^{-1} are attributed to residual electrolyte. The volume change in lithiation/delithiation processes leads surface of the Sn–Co alloy thin film electrode to be cracked and pulverized. EC, which is solid and nonvolatile at room temperature, probably trapped in the powdery surface films. It is difficult to eliminate electrolyte completely from the surface by rinsing and evacuating. The bands at 1644 cm^{-1} ($\upsilon_{as,C=O}$), 1484–1467 cm^{-1} (δ_{C-H}), 1300 cm^{-1} ($\upsilon_{s,C=O}$), 1116 cm^{-1} (υ_{C-O}) and 842 cm^{-1} (δoc-oo−) suggest that the main composition of SEI layer is $ROCO_2Li$ on a cycled Sn–Co alloy anode in 1 M $LiPF_6$/EC + DMC (1:1, vol.%), i.e. one of the reductive products of EC [28,29].

4. Conclusions

The current study puts emphasis upon investigation of the interfacial properties of Sn–Co alloy film anode with a high IR reflectivity by in situ MFTIRS at molecular level. Sn–Co alloy thin film electrode with an atomic ratio of 2:1 was prepared by electroplating. The lithiation/delithiation processes on Sn–Co anode are probed clearly by in situ MFTIRS, through the solvation/desolvation effects. The solvation/desolvation of lithium ions with solvent molecule of electrolyte leads to the variations of concentration of free solvent molecules (EC, DMC) and solvated solvent molecules ($Li(sol)_n^+$) in the thin layer between IR windows and electrode in the lithiation/delithiation processes, and induces IR bands shifts between free solvent molecule and $Li(sol)_n^+$ species. In comparison with free solvent molecule, the bond of C═O in $Li(sol)_n^+$ is weakened by the coordination of $Li^{+\cdots}O{=}C$, its asymmetric stretching frequency ($\upsilon_{as,C=O}$) is red-shifted, while the bond of C–O is strengthened by this coordination, which is consequently blue-shifted. The shifts of C═O, C–O bands were observed and measured. Ex situ MFTIRS studies of a cycled Sn–Co alloy thin film electrode in 1 M $LiPF_6$/EC + DMC have determined that the SEI layer is composed of mainly $ROCO_2Li$ species.

Acknowledgments

This study was subsidized by the Special Funds for Major State Basic Research Project of China (Grant No. 2009CB220102) and NSFC (Grant Nos. 20833005, 20773102 and 20910088).

References

[1] M. Winter, J.O. Besenhard, Electrochimica Acta 45 (1999) 31–50.
[2] N.C. Li, C.R. Martin, B. Scrosati, Journal of Power Sources 97–98 (2001) 240–243.
[3] I. Grigoriants, L. Sominski, H.L. Li, I. Ifargan, D. Aurbach, A. Gedanken, Chemical Communications 7 (2005) 921–923.
[4] A.D.W. Todd, R.A. Dunlap, J.R. Dahn, Journal of Alloys and Compounds 443 (2007) 114–120.
[5] J. Hassoun, S. Panero, P. Simon, P.L. Taberna, B. Scrosati, Advanced Materials 19 (2007) 1632–1635.
[6] F.S. Ke, L. Huang, J.S. Cai, S.G. Sun, Electrochimica Acta 52 (2007) 6741–6747.
[7] J.O. Besenhard, J. Yang, M. Winter, Journal of Power Sources 68 (1997) 87–90.
[8] R.C. Alkire, D.M. Kolb, J. Lipkowski, P.N. Ross (Eds.), Diffraction and Spectroscopic Methods in Electrochemistry, Wiley-VCH Verlag, Weinheim, 2006, pp. 315–376.
[9] D. Ostrovskii, F. Ronci, B. Scrosati, P. Jacobsson, Journal of Power Sources 103 (2001) 10–17.
[10] D. Aurbach, B. Markovsky, A. Shechter, Y. EinEli, H. Cohen, Journal of the Electrochemical Society 143 (1996) 3809–3820.
[11] D. Aurbach, B. Markovsky, A. Rodkin, M. Cojocaru, E. Levi, H.J. Kim, Electrochimica Acta 47 (2002) 1899–1911.

[12] A. Naji, J. Ghanbaja, B. Humbert, P. Willmann, D. Billaud, Journal of Power Sources 63 (1996) 33–39.
[13] L. Gireaud, S. Grugeon, S. Laruelle, S. Pilard, J.M. Tarascon, Journal of the Electrochemical Society 152 (2005) A850–A857.
[14] S.W. Song, S.W. Baek, Electrochimica Acta 54 (2009) 1312–1318.
[15] K. Morigaki, Journal of Power Sources 103 (2002) 253–264.
[16] H.J. Santner, C. Korepp, M. Winter, J.O. Besenhard, K.C. Moller, Analytical and Bioanalytical Chemistry 379 (2004) 266–271.
[17] T. Matsushita, K. Dokko, K. Kanamura, Journal of Power Sources 146 (2005) 360–364.
[18] P. Novak, D. Goers, L. Hardwick, M. Holzapfel, W. Scheifele, J. Ufhiel, A. Wursig, Journal of Power Sources 146 (2005) 15–20.
[19] Y. Ikezawa, T. Ariga, Electrochimica Acta 52 (2007) 2710–2715.
[20] D. Aurbach, M. Moshkovich, Y. Cohen, A. Schechter, Langmuir 15 (1999) 2947–2960.
[21] J.T. Li, S.R. Chen, X.Y. Fan, L. Huang, S.G. Sun, Langmuir 23 (2007) 13174–13180.
[22] A.D.W. Todd, R.E. Mar, J.R. Dahn, Journal of the Electrochemical Society 153 (2006) A1998–A2005.
[23] T. Fukushima, Y. Matsuda, H. Hashimoto, R. Arakawa, Electrochemical and Solid-State Letters 4 (2001) A127–A128.
[24] Y.X. Wang, P.B. Balbuena, International Journal of Quantum Chemistry 102 (2005) 724–733.
[25] M. Masia, M. Probst, R. Rey, Journal of Physical Chemistry B 108 (2004) 2016–2027.
[26] H.L. Yeager, J.D. Fedyk, R.J. Parker, Journal of Physical Chemistry 77 (1973) 2407–2410.
[27] H. Yoshida, T. Fukunaga, T. Hazama, M. Terasaki, M. Mizutani, M. Yamachi, Journal of Power Sources 68 (1997) 311–315.
[28] J.Z. Li, H. Li, Z.X. Wang, X.J. Huang, L.Q. Chen, Journal of Power Sources 81–82 (1999) 346–351.
[29] C.R. Wang, Y.Y. Wang, C.C. Wan, Journal of Power Sources 72 (1998) 66–70.